ACTA IMEKO
ISSN: 2221-870X
June 2026, Volume 15, Number 2, 1 - 8

Structure–property–migration relationships in polyethylene food packaging: FTIR classification, DSC crystallinity, and UV-absorbing contaminants in ethanol simulants

Anne C. Alcantara[1], Josefino A. Mendoza[1], Vince Z. Tabao[1], Elyson Keith P. Encarnacion[1], Rizel Marie S. M. Ting[1], Winnie P. Alejandro[1], Agaseve F. Del Rosario[1], David J. Alcarde Jr.[1]

[1] *Department of Science and Technology, Industrial Technology Development Institute, Packaging Technology Division, Packaging Safety Laboratory, Bicutan, Taguig City, Philippines*

ABSTRACT
Polyethylene films are widely used as food-contact packaging materials, yet migration behaviour can vary depending on polymer structure, thermal properties, and food simulant conditions. This study evaluated the migration of UV-absorbing contaminants from commercially available polyethylene packaging films, using an integrated structure–property–migration approach. Fourteen polyethylene films collected from the local market were classified as LDPE-like or HDPE-like based on FTIR spectral features associated with chain structure, while thermal behaviour and degree of crystallinity were determined using differential scanning calorimetry. Preliminary migration screening was conducted using ethanol-based food simulants under controlled conditions, with 20 % ethanol applied as a more aggressive simulant relative to the earlier screening performed using 8 % ethanol. Migration responses were assessed using UV–VIS spectrophotometry as a comparative screening tool. FTIR and DSC analyses revealed substantial structural and thermal variability among the films, with crystallinity values ranging from approximately 10 % to 50 %. Migration screening responses showed broader variability among some lower-crystallinity films, however, exploratory analysis indicated that crystallinity alone did not fully explain the observed responses. Overall, the findings demonstrate the complexity of structure–property–migration relationships in commercial polyethylene packaging films, and highlight the value of integrating spectroscopic, thermal, and screening-based analytical approaches for comparative migration evaluation.

Section: RESEARCH PAPER

Keywords: polyethylene packaging; migration screening; FTIR spectroscopy; differential scanning calorimetry; UV–VIS spectrophotometry

Citation: A. C. Alcantara, J. A. Mendoza, V. Z. Tabao, E. K. P. Encarnacion, R. M. S. M. Ting, W. P. Alejandro, A. F. Del Rosario, D. J. Alcarde Jr. , Structure–property–migration relationships in polyethylene food packaging: FTIR classification, DSC crystallinity, and UV-absorbing contaminants in ethanol simulants, Acta IMEKO, vol. 15 (2026) no. 2, pp. 1-8. DOI: 10.21014/actaimeko.v15i2.2286

Section Editor: Leonardo Iannucci, Politecnico di Torino, Italy

Received January 12, 2026; **In final form** June 16, 2026; **Published** June 2026

Funding: This work was supported by the Industrial Technology Development Institute (DOST-ITDI) through the General Appropriations Act (GAA) and by the Department of Science and Technology (DOST) through the Grants-in-Aid (GIA) Program, Philippines.

Corresponding author: Anne Alcantara, e-mail: acalcantara@itdi.dost.gov.ph

1. INTRODUCTION

Polyethylene (PE) films dominate the food-contact packaging materials because they are cheap, flexible, and readily available [1], [2], [3]. Both low-density polyethylene (LDPE) and high-density polyethylene (HDPE) films see extensive use in retail and informal food supply chains, particularly across developing and tropical regions [4]. While PE itself is chemically stable, the commercial films we actually encounter contain additives, stabilizers, or non-intentionally added substances (NIAS) that can migrate into food during use [2], [5], [6]. Ultraviolet (UV)-absorbing contaminants pose a specific concern, as these compounds, which may originate from stabilizing agents or degradation products, have been linked to potential health and environmental risks [7]. Given these risks, understanding how substances migrate from PE packaging into food products continues to be essential for protecting consumers [2].

Several structural and physicochemical factors are influenced by migration from polyethylene (PE) food-contact materials. PE has a semicrystalline structure characterized by crystalline lamellae embedded within amorphous zones [3], [8]. Molecular movement is constrained within the crystalline regions, whereas

the amorphous areas create easier routes for diffusion [3], [8]. This means that polymer density, the extent to which the chains branch, and crystallinity levels all matter when predicting migration [3], [8]. Studies have repeatedly demonstrated that LDPE exhibits faster diffusion and greater migration than HDPE does, which makes sense given their structural differences—LDPE possesses less ordered chains and a more loosely organized crystalline structure [3], [8], [9], [10]. Because of this connection, we routinely use differential scanning calorimetry (DSC) data, like melting temperature and crystallinity percentage, as indirect predictors of the migration potential [3], [8], [11].

Understanding PE morphology is essential for interpreting how substances move through it. The chemical composition of test simulants also shapes what we observe in migration tests. Ethanol-based simulants are commonly used to represent contact conditions for aqueous, alcoholic, and certain fatty or semi-polar food systems, and they are effective at extracting UV-absorbing migrants from PE materials [12]. Changing the ethanol concentration alters the partitioning behavior between the polymer and the simulant, which can influence the apparent migration response. In addition, polymer–simulant interactions associated with changes in simulant polarity may also affect diffusion behavior and mass kinetics within the polymer matrix [13], [14]. Despite this, many migration studies rely on a single simulant concentration, which limits the ability to examine the role of simulant polarity under otherwise comparable conditions [14], [15].

UV–VIS spectrophotometry offers a quick way to screen for total UV-absorbing contaminants from food-contact plastics [16], [17], [18]. Chromatography and mass spectrometry can identify specific compounds, but they are expensive and time-consuming for routine work [19]. Screening methods, when used appropriately, give us a practical option for comparing many samples and for building tiered assessment strategies [20].

At an earlier conference, the authors validated a UV–VIS spectrophotometric screening method and applied it to PE films using a single ethanol-based food simulant [21]. That work used Fourier transform infrared (FTIR) analysis to identify polymer through library matching, while the detailed interpretation of chain structure, crystallinity, and simulant polarity effects was outside the study scope. So, the relationships between polymer structure, thermal behavior, and migration response were not thoroughly examined.

The present study builds on that foundation with a more complete structure–property–migration approach. Polymer films were collected from the local market and FTIR spectroscopy was used to classify them as LDPE-like and HDPE-like behavior based on their spectral features. Thermal properties and the degree of crystallinity were determined by differential scanning calorimetry (DSC), and migration of UV-absorbing contaminants was evaluated using ethanol-based food simulants of different concentrations. Bringing together structural characterization, thermal analysis, and migration screening within a single dataset allows us to better understand migration behavior in real-world PE packaging, and shows how simulant polarity affects what we detect.

In this study, the objective was to evaluate the migration behavior of UV-absorbing contaminants from commercially available PE food-contact films, using an integrated structure–property–migration approach. Specifically, the study aimed to (i) classify market-sourced PE films as LDPE-like or HDPE-like, using FTIR chain structure indicators, (ii) measure thermal behavior and the degree of crystallinity using DSC, (iii) test UV-absorbing contaminant migration using ethanol-based food simulants of different concentrations under controlled conditions, and (iv) evaluate the relationships between polymer structural and thermal characteristics and the observed migration response of UV-absorbing contaminants during screening analysis. By combining structural, thermal, and migration data within a single experimental framework, the study seeks to clarify the influence of polymer morphology and simulant polarity on migration trends observed during migration screening.

The paper proceeds as follows: Section 2 describes the materials and experimental procedures. Section 3 presents and discusses the results of FTIR-based structural classification, DSC thermal analysis, and UV–VIS migration screening, including the integrated structure–property–migration relationships. Finally, Section 4 summarizes the main conclusions and implications for polyethylene packaging safety assessment.

2. MATERIALS AND METHODS

2.1. Materials and sample selection

Fourteen (14) polyethylene (PE) packaging films were selected from the sample set analyzed in the earlier conference study [21]. These samples consisted of commercially available, single-use, flexible films collected from different brands in the Philippine market and commonly used for food-contact applications. The PE films used in the migration screening experiments had thicknesses ranging from approximately 6-130 μm [21]. The subset was chosen to represent distinct products while avoiding redundancy among similar samples, allowing focused comparison of material variability across brands.

The same samples were used in the present work to enable a direct comparison between migration results obtained using 8 % ethanol and those obtained using 20 % ethanol under identical test conditions.

Prior to analysis, all samples were visually inspected and cut into appropriate dimensions suitable for FTIR-ATR contact, DSC pan loading, and UV–VIS analysis. Each PE film was identified using a unique sample code (PE-0001 to PE-0014), consistent with the coding scheme used in the earlier migration screening study, to ensure traceability and facilitate comparison across analyses.

2.2. FTIR spectroscopic analysis

FTIR spectroscopy was used to confirm polymer identity and to classify the PE films based on structural features. FTIR measurements were performed using a Shimadzu IR-Prestige-21 spectrometer equipped with an attenuated total reflectance (ATR) accessory. Spectra were acquired over the spectral range of 4000–400 cm^{-1} at a resolution of 4 cm^{-1}, with 32 scans per sample to ensure an adequate signal-to-noise ratio.

PE identity was verified through the presence of characteristic absorption bands associated with C–H stretching and deformation modes, which are well established for polyolefin materials [22], [23], [27], [28]. Structural classification of the films into LDPE-like and HDPE-like groups was based on qualitative interpretation of FTIR spectral features related to chain branching and crystallinity. These included the relative prominence of CH_3 bending bands, CH_2 deformation bands, and the position and sharpness of the CH_2 rocking region, which have been reported to reflect differences in chain structure and crystalline order in PE [23], [29], [30], [31].

2.3. Differential scanning calorimetry (DSC): Thermal characterization and crystallinity determination

DSC was employed to evaluate the thermal behavior and degree of crystallinity of the PE films. Measurements were carried out using a Shimadzu DSC-60A under a nitrogen atmosphere to minimize oxidative effects during heating. Approximately 5–6 mg of each PE film was sealed in standard aluminum DSC pans, with an empty pan used as the reference.

Samples were heated at a constant rate of 10 °C min^{-1} from approximately 50 °C to 170 °C. Within this scan range, the melting endotherm of PE, which typically occurs between approximately 105 and 135 °C depending on chain structure and crystallinity, was fully captured °C [25], [32]. The melting temperature (T_{m}) was determined from the peak maximum of the endothermic transition, while the enthalpy of fusion (ΔH_{m}) was obtained from the integrated area under the melting peak [26].

The degree of crystallinity ($\%Xc$) was calculated using the relationship:

$$\%Xc = \frac{\Delta Hf}{\Delta H°f} \cdot 100\,, \tag{1}$$

where $\Delta H°f$ = 293 J g^{-1} represents the enthalpy of fusion of 100 % crystalline PE [3].

2.4. UV–Vis migration screening using ethanol food simulants

Migration screening was conducted using ethanol-based food simulants under conditions adapted from the U.S. FDA 21 CFR Part 177 for the screening-level evaluation of food-contact packaging materials [33]. Ethanol–water mixtures of 8 % and 20 % (v/v) were employed to represent food simulants of differing polarities.

Migration data obtained using 8 % ethanol were previously reported as part of an earlier screening study [21]. In the present work, 20 % ethanol was applied to extend the comparative assessment and to examine migration behavior under a higher ethanol concentration. The results reported here are based on preliminary screening measurements and are intended for the comparative evaluation of migration trends among samples and between simulant conditions, rather than for compound-specific quantification or regulatory compliance assessment.

Film samples were exposed to the simulant at 49 °C for 24 hours under controlled conditions. To minimize variability associated with the exposed contact area, all migration tests were performed using a constant film surface area-to-simulant ratio of 50 cm² film per 100 mL simulant under identical extraction conditions. Following exposure, the simulant solutions were collected and analyzed using UV–VIS spectrophotometry. Measurements were performed using a Shimadzu UV-1800 double-beam spectrophotometer, with absorbance spectra recorded in absorbance mode over the wavelength range of 220-360 nm using 5 cm quartz cuvettes.

Prior to the analysis of each sample, the instrument was zeroed using the corresponding reagent blank prepared under identical conditions.

2.5. Data interpretation and analysis

Data obtained from FTIR spectroscopy, DSC, and UV–VIS spectrophotometry were interpreted using an integrated structure–property–migration framework. In particular, FTIR-based polymer classification and DSC-derived thermal parameters were examined alongside UV–VIS migration screening results, to explore potential relationships between polymer structure, thermal behavior, and migration response across the analyzed PE films. FTIR results were used to classify PE films as LDPE-like or HDPE-like, based on qualitative spectral characteristics associated with chain branching and crystalline organization. DSC parameters, including melting temperature and the degree of crystallinity, were used to describe thermal behavior and support the interpretation of polymer morphology.

UV–VIS absorbance values were treated as preliminary screening indicators, and used for the comparative evaluation of migration behavior among samples and between ethanol simulant concentrations. Absorbance measurements were performed in duplicate, and reported values represent the mean of the two measurements. The interpretation focused on the relative differences in absorbance rather than the absolute quantification of migrated species. Although the exposed surface area-to-simulant ratio was standardized during extraction, the absorbance values were compared directly without thickness correction. Therefore, film thickness and material morphology may have contributed to the observed migration response, and the results should be interpreted as comparative screening values rather than thickness-normalized migration measurements.

Migration trends were examined in relation to polymer structural classification and crystallinity, to identify general patterns across the sample set. As DSC measurements were conducted once per sample and UV–VIS analysis was based on duplicate measurements, the integrated interpretation was considered exploratory in nature. The relationships between structure, thermal behavior, and migration response were therefore interpreted as associative trends rather than definitive causal relationships.

No compound-specific identification or regulatory compliance assessment was performed. The combined interpretation was intended to provide a comparative framework for understanding migration screening behavior in PE packaging films under controlled test conditions.

3. RESULTS AND DISCUSSION

3.1. FTIR-based structural classification of PE packaging films

Clear structural variability was observed among the PE packaging films, despite all samples exhibiting the characteristic infrared features of PE. Differences in peak definition and relative intensity indicated variations in chain structure and molecular organization across the sample set.

All spectra displayed the expected PE absorption features, including C–H stretching and deformation bands, confirming the polymer backbone. Despite these shared characteristics, noticeable differences were evident in the sharpness of deformation bands, and in the position and definition of the CH_2 rocking region (Figure 1), which provided the basis for structural differentiation among samples.

Based on the combined spectral characteristics, the films were classified into LDPE-like and HDPE-like groups, as summarized in Table 1. LDPE-like samples (PE-0001, PE-0002, PE-0003, PE-0005, PE-0006, and PE-0008) exhibited broader deformation features within the CH_2 bending region (~1460-1470 cm^{-1}), together with less well-defined rocking bands within the lower wavenumber region near ~717–721 cm^{-1}. These spectral features are commonly associated with increased chain branching and lower apparent crystalline order. In contrast, HDPE-like samples (PE-0004, PE-0007, and PE-0009 to PE-0014) displayed sharper and more defined deformation

Table 1. Summary of FTIR spectral features used for the structural classification of PE packaging films.

Sample ID	CH_3 bend (~1370 cm^{-1})	CH_2 deformation region (~1460–1470 cm^{-1})	CH_2 rocking (~717–731 cm^{-1})	Structural feature	Polymer group
PE-0001	More pronounced	Broader / less defined	~721	Branched / lower apparent crystalline order	LDPE-like
PE-0002	More pronounced	Broader / less defined	~717	Branched / lower apparent crystalline order	LDPE-like
PE-0003	More pronounced	Broader / less defined	~717	Branched / lower apparent crystalline order	LDPE-like
PE-0004	Less pronounced	Sharper / more defined	~731	More linear / higher apparent crystalline order	HDPE-like
PE-0005	More pronounced	Broader / less defined	~717	Branched / lower apparent crystalline order	LDPE-like
PE-0006	More pronounced	Broader / less defined	~717	Branched / lower apparent crystalline order	LDPE-like
PE-0007	Less pronounced	Sharper / more defined	~731	More linear / higher apparent crystalline order	HDPE-like
PE-0008	More pronounced	Broader / less defined	~717	Branched / lower apparent crystalline order	LDPE-like
PE-0009	Less pronounced	Sharper / more defined	~731	More linear / higher apparent crystalline order	HDPE-like
PE-0010	Less pronounced	Sharper / more defined	~731	More linear / higher apparent crystalline order	HDPE-like
PE-0011	Less pronounced	Sharper / more defined	~731	More linear / higher apparent crystalline order	HDPE-like
PE-0012	Less pronounced	Sharper / more defined	~731	More linear / higher apparent crystalline order	HDPE-like
PE-0013	Less pronounced	Sharper / more defined	~731	More linear / higher apparent crystalline order	HDPE-like
PE-0014	Less pronounced	Sharper / more defined	~731	More linear / higher apparent crystalline order	HDPE-like

bands along with more distinct rocking features toward the higher-wavenumber region near ~730–731 cm^{-1}, indicative of more linear chain structures and higher crystalline order. The classification was therefore based on overall spectral profile interpretation rather than the isolated presence or absence of a single absorption band [34].

Although PE-0008 exhibited LDPE-like FTIR features, it is discussed in later sections as a borderline or mixed case based on its thermal behavior, highlighting the complementary nature of spectroscopic and thermal analyses. The overlap in crystallinity values observed for certain samples (e.g., PE-0004 and PE-0005) further indicates that no single crystallinity threshold can reliably distinguish LDPE-like from HDPE-like films within commercially produced PE materials. Therefore, the structural classification in the present study was based primarily on comparative FTIR spectral interpretation, with DSC results used as complementary thermal characterization data.

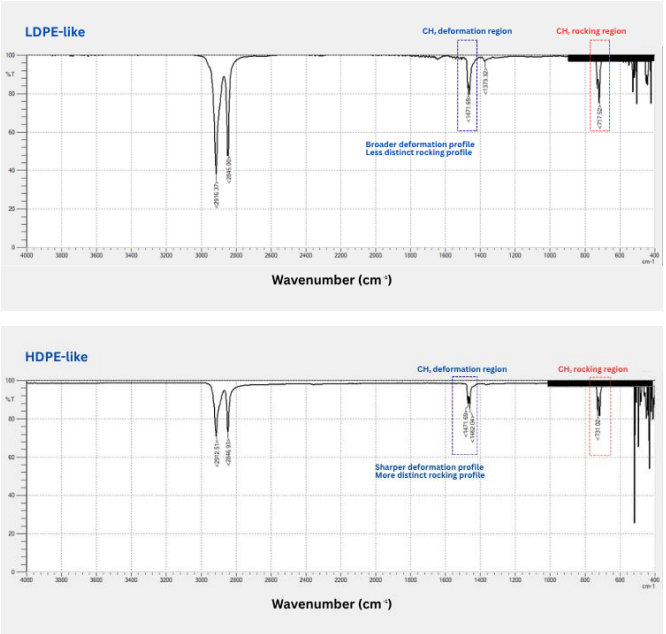

Figure 1. Representative FTIR-ATR spectra of LDPE-like and HDPE-like polyethylene packaging films, illustrating differences in the overall spectral profile, particularly within the CH_2 deformation and rocking regions, used for comparative structural classification.

Overall, the FTIR results demonstrate that PE packaging films marketed under different brands are not structurally uniform, despite being nominally identified as PE. The resulting LDPE-like and HDPE-like classification provides a structural framework for interpreting the thermal behavior and migration screening results discussed in the following sections, in line with structure–property relationships reported for PE packaging materials [8].

3.2. Thermal behavior and crystallinity of PE films by DSC

Clear differences in melting behavior and crystallinity were observed among the PE packaging films. All samples exhibited melting endotherms within the temperature range typically reported for PE, with peak melting temperatures ranging from approximately 107 to 131 °C (Table 2), consistent with materials differing in chain structure and crystalline organization [35], [36].

The peak melting temperature (T_m), enthalpy of fusion (ΔH_f), and calculated degree of crystallinity ($\%Xc$) are summarized in Table 2. Samples classified as LDPE-like generally exhibited lower and more dispersed crystallinity values, ranging from 10.4 % to 31.7 %. For example, PE-0002 showed the lowest crystallinity (10.4 %), while PE-0005 and PE-0006 exhibited intermediate values (31.7 % and 28.2 %, respectively). This wider spread in $\%Xc$ is consistent with greater heterogeneity in crystalline organization, which is commonly associated with branched PE systems [35].

In contrast, HDPE-like samples displayed consistently higher crystallinity values, typically between 45.2 % and 50.1 %. Samples such as PE-0009, PE-0010, and PE-0014 exhibited $\%Xc$ values close to or exceeding 49 %, together with peak melting temperatures clustered around 129–130 °C, suggesting more uniform crystalline domains and higher chain regularity.

Differences in melting peak shape were further supported by the onset and end melting temperatures provided in Supplementary Table S1. LDPE-like samples generally showed wider onset-to-end temperature ranges, indicating broader melting endotherms associated with a distribution of crystalline

Table 2. The DSC melting temperature (T_m), enthalpy of fusion (ΔH_f), and degree of crystallinity (%Xc) of PE packaging samples.

Sample ID	Peak T_m (°C)	ΔH_f (J/g)	%Xc (%)
PE-0001	121.29	74.41	25.4
PE-0002	107.37	30.51	10.4
PE-0003	121.9	44.96	15.3
PE-0004	130.81	104.26	35.6
PE-0005	120.66	92.79	31.7
PE-0006	109.11	82.55	28.2
PE-0007	129.24	136.69	46.6
PE-0008	114.32 / 120.31	19.87	6.8
PE-0009	129.26	142.13	48.5
PE-0010	130.04	146.69	50.1
PE-0011	129.77	145.49	49.6
PE-0012	129.38	132.5	45.2
PE-0013	130.01	136.62	46.6
PE-0014	129.57	146.22	49.9

domains of varying thermal stability. In contrast, HDPE-like samples exhibited narrower melting intervals, consistent with more uniform crystalline populations.

A notable exception was PE-0008, which exhibited a bimodal melting behavior, with two overlapping peak temperatures at approximately 114 and 120 °C. Such bimodal endotherms are commonly associated with PE blends or materials containing multiple crystalline populations with different lamellar thicknesses [37]. This behavior suggests a mixed PE structure, consistent with its borderline classification in the FTIR analysis.

Overall, the DSC results corroborate the FTIR-based structural classification presented in Section 3.1. LDPE-like films were associated with lower and more variable crystallinity and broader melting behavior, while HDPE-like films exhibited higher and more tightly clustered crystallinity values with sharper melting transitions. These differences in crystalline organization are relevant to migration behavior, as the diffusion of low-molecular-weight species is generally favoured in amorphous regions, and may be influenced by the presence of heterogeneous crystalline structures. The implications of these thermal properties for migration screening are discussed in the following section.

3.3. Migration screening of UV-absorbing contaminants using ethanol food simulants

Migration screening using ethanol food simulants revealed material-dependent differences in UV-absorbing responses among the PE films. When compared under identical temperature (49 °C) and exposure time (24 h) conditions, the use of 20 % ethanol generally resulted in higher or more readily detectable absorbance responses than 8 % ethanol, indicating enhanced screening sensitivity under higher ethanol concentration. Higher ethanol concentrations are known to provide a more aggressive simulant environment, enhancing polymer–simulant interactions and the release of potential migrant species from polyolefin materials [38].

The blank-corrected UV–VIS absorbance values measured in the 220–360 nm range are summarized in Table 3. Several samples that showed near-zero or very low absorbance in 8 % ethanol (e.g., PE-0001, PE-0004, and PE-0010) showed measurable responses when exposed to 20 % ethanol, supporting the use of higher ethanol concentrations as a more sensitive screening medium for differentiating material behavior.

However, the response across the sample set was not uniform. Some films exhibited comparable or lower absorbance values at 20 % ethanol compared to 8 % ethanol (e.g., PE-0003 and PE-0005), indicating that migration screening responses are influenced not only by simulant polarity but also by material-specific factors. These include polymer structure, crystallinity, and possible formulation differences, as discussed in Sections 3.1 and 3.2.

When considered alongside the FTIR and DSC results, films classified as LDPE-like tended to exhibit a wider range of absorbance responses, including some of the higher values observed under 20 % ethanol exposure (e.g., PE-0002 and PE-0008). This broader response range is consistent with the lower apparent crystalline order and greater structural heterogeneity identified for these films, which may facilitate the diffusion of UV-absorbing species. In contrast, HDPE-like films generally exhibited lower or more tightly clustered absorbance values, although measurable responses were still observed for several samples (e.g., PE-0009), highlighting the influence of additional material parameters beyond crystallinity alone.

Overall, the UV–VIS results demonstrate that increasing ethanol concentration enhances the sensitivity of migration screening and reveals material-dependent differences among PE films. While this screening approach does not provide compound-specific quantification or regulatory compliance assessment, it effectively highlights relative migration tendencies that can be interpreted in the context of polymer structure and thermal properties.

3.4. Structure–property–migration relationships in PE films

The combined FTIR, DSC, and UV–VIS results were integrated to examine the structure–property–migration relationships among the analyzed PE films. Figure **3** compares the distribution of UV–VIS migration screening responses between films classified as LDPE-like and HDPE-like, based on FTIR interpretation. LDPE-like films generally exhibited a wider

Table 3. Blank-corrected UV–VIS preliminary screening absorbance values (220–360 nm) of PE films after exposure to 8 % and 20 % ethanol at 49 °C for 24 h.

Sample ID	Absorbance_Au (8% Ethanol)	Absorbance_Au (20% Ethanol)
PE-0001	0.000	0.017
PE-0002	0.003	0.028
PE-0003	0.009	0.001
PE-0004	0.000	0.002
PE-0005	0.093	0.004
PE-0006	0.001	0.001
PE-0007	0.000	0.004
PE-0008	0.154	0.022
PE-0009	0.007	0.036
PE-0010	0.000	0.014
PE-0011	0.005	0.002
PE-0012	0.015	0.008
PE-0013	0.005	0.015
PE-0014	0.002	0.007

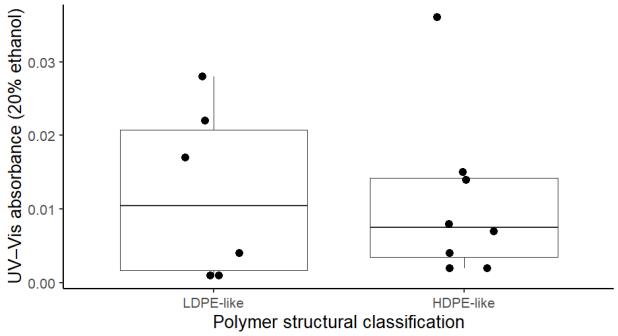

Figure 2. Distribution of UV–VIS migration screening responses for LDPE-like and HDPE-like PE films after exposure to 20 % ethanol (49 °C, 24 h). The points represent individual film samples; the boxplot summarizes the spread of absorbance values.

spread of absorbance responses, whereas HDPE-like films tended to cluster within lower absorbance ranges. This distribution generally aligns with established polymer structure-property concepts, where chain branching and lower apparent crystalline order may contribute to an increased variability in migration screening responses. However, the overlap between LDPE-like and HDPE-like samples indicates that migration behavior was also influenced by additional material-related factors beyond crystallinity alone [39], [40], [41], [42].

To further explore the relationship between thermal properties and migration behavior, the UV–VIS absorbance values obtained using 20 % ethanol were compared with the degree of crystallinity determined by DSC (Figure 3). Although some lower crystallinity films exhibited relatively higher absorbance responses and greater variability, exploratory Spearman correlation analysis showed no significant monotonic relationship between crystallinity and migration screening responses ($\rho = -0.052$, $p = 0.860$). These results suggest that crystallinity alone did not govern the observed migration behavior within the analyzed sample set. Instead, the broader variability observed among lower-crystallinity films may reflect the combined influence of polymer morphology, additive composition, processing history, and molecular weight distribution commonly present in commercial PE materials.

The influence of polymer structure became even more evident when individual samples were considered. For example, PE-0008, which exhibited a bimodal melting behavior and intermediate crystallinity, showed relatively high absorbance values under both 8 % and 20 % ethanol exposure. In contrast, more crystalline HDPE-like samples, such as PE-0011 and PE-0014, generally exhibited lower absorbance values under the same extraction conditions. Such variability likely reflects the combined influence of additive composition, processing history, molecular weight distribution, and crystalline morphology commonly observed in commercial PE films [10].

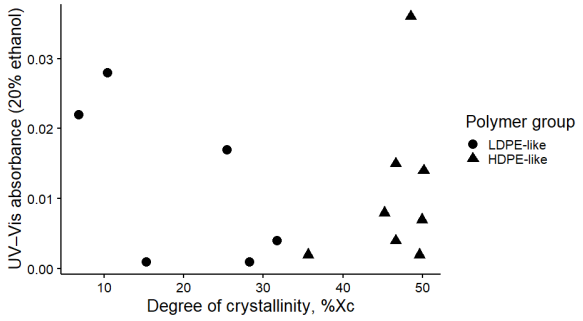

Figure 3. UV–VIS absorbance (20% ethanol, 49 °C for 24 h) as a function of PE film crystallinity (%Xc) determined by DSC. Points represent individual film samples classified as LDPE-like or HDPE-like based on FTIR interpretation.

Taken together, the migration screening results demonstrate that both simulant polarity and material-specific structural characteristics contributed to the observed UV-absorbing responses among PE films. Although the present study was limited to screening-level evaluation and did not provide a compound-specific quantification or regulatory compliance assessment, the integrated FTIR, DSC, and UV–VIS results offer a practical framework for the comparative interpretation of migration screening trends in PE food-contact materials.

4. CONCLUSIONS

This study demonstrated that PE food packaging films sold under different brands exhibit measurable differences in polymer structure, thermal behavior, and migration screening response, despite being nominally identified as PE. FTIR analysis enabled the classification of the films into LDPE-like and HDPE-like groups, based on established spectral features associated with chain branching and crystalline order. Differential scanning calorimetry further confirmed these distinctions by revealing systematic differences in melting behavior and the degree of crystallinity, including the identification of films with mixed or bimodal crystalline populations.

Migration screening using UV–VIS spectrophotometry showed that increasing ethanol concentration from 8 % to 20 % enhanced the sensitivity of the screening method and revealed material-dependent differences in UV-absorbing responses. When interpreted together, the FTIR, DSC, and UV–VIS results suggested that films with a lower apparent crystallinity and more heterogeneous structures tended to exhibit a broader variability in migration screening responses. However, exploratory statistical analysis indicated that crystallinity alone did not show a significant monotonic relationship with the absorbance response, highlighting the influence of additional material-related factors in commercial PE films.

Although the present work was limited to screening-level evaluation and did not involve a compound-specific quantification or regulatory compliance assessment, the integrated structure–property–migration framework provides a practical approach for the comparative evaluation of PE packaging materials. The findings highlight the importance of considering polymer structure and thermal properties when interpreting migration screening results, and support the use of complementary analytical techniques for the preliminary assessment of food-contact materials.

ACKNOWLEDGEMENT

The authors gratefully acknowledge the Department of Science and Technology (DOST), through the Philippine Council for Industry, Energy and Emerging Technology Research and Development (PCIEERD), for its monitoring support and guidance in ensuring the timely implementation and completion of the project deliverables. The authors also thank the laboratory personnel of the Industrial Technology Development Institute (ITDI) for their technical assistance during sample preparation and instrumental analyses.

REFERENCES

[1] I. Novák, A. Popelka, Z. Špitalský, I. Krupa, Ş. Tavman, Polyolefin in packaging and food industry, Springer, 2016
DOI: 10.1007/978-3-319-25982-6_7

[2] R. K. Gupta, S. Pipliya, S. Karunanithi, G. M. Eswaran U, S. Kumar, S. Mandliya, P. P. Srivastav, T. Suthar (+ 3 more authors), Migration of chemical compounds from packaging materials into packaged foods: interaction, mechanism, assessment, and regulations, Foods 13 (2024) 19, 3125.
DOI: 10.3390/foods13193125

[3] L. C. Bolte, H. Gers-Barlag, G. Heinsohn, R. Daniels, Migration of cosmetic components into polyolefins, Advances in Polymer Technology 2024 (2024), 2680899.
DOI: 10.1155/adv/2680899

[4] M. D. Ruiz Medina, J. Ruales, Physicochemical and mechanical characterization of HDPE and LDPE films used in the postharvest packaging of banana (*Musa paradisiaca*). Online [Accessed 7 January 2026]
DOI: 10.20944/preprints202509.1156.v1

[5] M. de S. Mesquita, S. de M. P. Abrantes, Potential antioxidant migration from polyethylene packaging to food: a systematic review, Polímeros – Ciência e Tecnologia 32 (2022) e20220081.
DOI: 10.1590/0104-1428.20220081

[6] Y. Wang, J. Wu, B. Liu, Y. Xia, Q. Lin, Migration of polymer additives and radiolysis products from irradiated PET/PE films into a food simulant, Food Control 124 (2021), 107886.
DOI: 10.1016/j.foodcont.2021.107886

[7] K. Matoušková, L. N. Vandenberg, UV screening chemicals, in: Reproductive and developmental toxicology, R. Gupta (editor), Academic Press, Oxford, 2022, ISBN 978-0-323-89773-0, pp. 1–15.
DOI: 10.1016/b978-0-323-89773-0.00045-x

[8] D. R. Sturm, K. J. Caputo, S. Liu, R. P. Danner, Diffusivity of solvents in semi-crystalline polyethylene using the Vrentas-Duda free-volume theory, Journal of Polymer Engineering 38 (2018), pp. 925–931.
DOI: 10.1515/polyeng-2018-0047

[9] J. Maia, A. Rodríguez-Bernaldo de Quirós, R. Sendón, J. M. Cruz, A. Seiler, R. Franz, C. Simoneau, L. Castle, (+ 5 more authors), Determination of key diffusion and partition parameters and their use in migration modelling of benzophenone from low-density polyethylene (LDPE) into different foodstuffs, Food Additives and Contaminants Part A 33 (2016), pp. 715–724.
DOI: 10.1080/19440049.2016.1156165

[10] Z. Maghsoud, M. Rafiei, M. H. N. Famili, Effect of processing method on migration of antioxidant from HDPE packaging into a fatty food simulant in terms of crystallinity, Packaging Technology and Science 31 (2018), pp. 141–149.
DOI: 10.1002/pts.2359

[11] N. Petrovics, C. Kirchkeszner, T. Tábi, N. Magyar, I. K. Székely, B. S. Szabó, Z. Nyiri, Zs. Eke, Effect of temperature and plasticizer content of polypropylene and polylactic acid on migration kinetics into isooctane and 95 v/v % ethanol as alternative fatty food simulants, Food Packaging and Shelf Life 33 (2022), 100916.
DOI: 10.1016/j.fpsl.2022.100916

[12] L. Wang, Z.-R. Li, L.-W. Chen, H.-Y. You, C.-S. Wu, W.-Q. Han, Y.-P. Xian, H.-Y. Luo, Simultaneous determination of migration amounts of the ultraviolet absorbers and antioxidants by ultra performance liquid chromatography in plastic food packaging materials, Journal of Food Safety and Quality 6 (2015), pp. 12–18. [In Chinese]
DOI: 10.19812/j.cnki.jfsq11-5956/ts.2015.12.007

[13] X. Huang, C. Hu, Z. Wang, Study on the migration of Irganox 1076 from HDPE into ethanol, Packaging Engineering 28 (2007), pp. 73–76. [In Chinese]
DOI: 10.3969/j.issn.1001-3563.2007.12.015

[14] Y. Ling, W. Yong, Y. Bian, M. He, M. Yao, F. Zhang, Y. Zhao, Study of the migration law of UV absorbants in polyethylene food contact materials based on deterministic migration model, Chinese Journal of Food Hygiene 33 (2021), pp. 421–426. [In Chinese]
DOI: 10.13590/j.cjfh.2021.06.016

[15] N. Petrovics, C. Kirchkeszner, A. Patkó, T. Tábi, N. Magyar, I. K. Székely, B. S. Szabó, Z. Nyiri, (+ 1 more author), Effect of crystallinity on the migration of plastic additives from polylactic acid-based food contact plastics. Online [Accessed 7 January 2026]
DOI: 10.2139/ssrn.4248603

[16] A. A. Barus, F. E. Appa, N. F. Bakri, M. E. Pratiwi, C. H. B. Tobi, Identification of bisphenol-A (BPA) in polycarbonate (PC) baby bottles in Jayapura, Papua, Sebatik 29 (2025) 1, pp. 122–128.
DOI: 10.46984/sebatik.v29i1.2570

[17] W. P. Alejandro, E. K. P. Encarnacion, A. C. Alcantara, D. J. Alcarde, H. E. Armario, A. F. D. Rosario, R. M. S. M. Ting, Assessment of total UV-absorbing contaminants in LDPE food packaging from Philippine markets, Current Research in Nutrition and Food Science 13 (2025).
DOI: 10.12944/crnfsj.13.2.26

[18] R. M. S. M. Ting, E. K. P. Encarnacion, A. C. Alcantara, D. J. Alcarde Jr., H. E. Armario, W. P. Alejandro, A. F. Del Rosario, A. S. L. Canonizado, Method validation and profiling of total UV-absorbing contaminants migrating from monolayered low-density polyethylene used for aqueous foods in the Philippines, Polyolefins Journal 12 (2025), pp. 357–371.
DOI: 10.22063/poj.2025.35740.1367

[19] Y. Sapozhnikova, Non-targeted analysis with liquid chromatography–high resolution mass spectrometry for the identification of food packaging migrants, Journal of Chromatography A 1676 (2022), 463215.
DOI: 10.1016/j.chroma.2022.463215

[20] M. Marin-Kuan, V. Pagnotti, A. Patin, J. Moulin, H. Latado, J. Varela, Y.-A. Hammel, Th. Gude, (+ 8 more authors), Interlaboratory study to evaluate a testing protocol for the safety of food packaging coatings, Toxics 11 (2023) 2, 156.
DOI: 10.3390/toxics11020156

[21] A. C. Alcantara, E. K. P. Encarnacion, R. M. S. M. Ting, W. P. Alejandro, H. E. Armario, A. F. D. Rosario, D. J. Alcarde Jr., Method validation and chemometric analysis of UV-absorbing contaminant migration from low-density polyethylene packaging materials into 8 % ethanol, Proc. of the 2025 IMEKO Joint Conf. TC8–TC11–TC25, Torino, Italy, 14–17 September 2025.
DOI: 10.21014/tc24-2025.038

[22] K. A. Prokhorov, G. Y. Nikolaeva, S. A. Gordeyev, P. P. Pashinin, D. P. Nikolaev, Raman scattering in oriented polyethylene: the C–H stretching region, Laser Physics 11 (2001), pp. 86–93.

[23] S. J. Spells, S. Coutry, Mixed crystal infrared spectroscopy of uniaxially drawn polyethylene films, Applied Spectroscopy 61 (2007), pp. 276–282.
DOI: 10.1366/000370207780220930

[24] B. Bamps, M. Buntinx, R. Peeters, Seal materials in flexible plastic food packaging: A review, Packaging Technology and Science 36 (2023), pp. 507–532.
DOI: 10.1002/pts.2732

[25] S. C. Shivasharana, S. S. Kesti, Physical and chemical characterization of low-density polyethylene and high-density polyethylene, Journal of Advanced Scientific Research 10 (2019), pp. 30–34. Online [Accessed 22 June 2026]
https://sciensage.info/index.php/JASR/article/view/309

[26] L. F. de Oliveira Junior, Z. de Oliveira Silvano, and P. M. Rocha, Thermal analysis of differential scan–DSC calorimetry for the pure high-density polyethylene and its variables, International Journal of Engineering Trends and Technology 65 (2018) 2, pp. 79–84.
DOI: 10.14445/22315381/IJETT-V65P215

[27] D. Zhang, G. Song, Study on infrared spectroscopy of polyethylene film material, Spectroscopy and Spectral Analysis 33 (2013), pp. 681–684. [In Chinese]
DOI: 10.3969/j.issn.1007-2934.2013.03.001

[28] M. Mohammadi, A. Azizi, Qualitative characterization of branches in various polyethylene species via Fourier transform

spectroscopy, in: Polymer Spectroscopy. Springer, Cham, 2018, pp. 344–347.
DOI: 10.1007/978-3-030-45085-4_82
[29] M. A. McRae, W. F. Maddams, Infrared spectroscopic studies on polyethylene, 2. the characterisation of specific types of alkyl branches in low-branched ethylene polymers and copolymers, Macromolecular Chemistry and Physics 177 (1976), pp. 449–459.
DOI: 10.1002/macp.1976.021770213
[30] P. C. Painter, J. Runt, M. M. Coleman, I. R. Harrison, Fourier-transform infrared study of polyethylene single crystals in suspension, Journal of Polymer Science Part B 15 (1977), pp. 1647–1654.
DOI: 10.1002/pol.1977.180150912
[31] N. Kang, Y. Xu, S. Weng, J. Wu, D. Xu, Effect of crystallization and branch on fine structure of orthorhombic polyethylene, Spectroscopy and Spectral Analysis 21 (2001), pp. 35–38. [In Chinese]
DOI: 10.3321/j.issn:1000-0593.2001.01.035
[32] B. Bamps, M. Buntinx, R. Peeters, Seal materials in flexible plastic food packaging: A review. Packaging Technology and Science, 36 (2023) 7, pp. 507–532.
DOI: 10.1002/pts.2732
[33] US Food and Drug Administration, Code of Federal Regulations Title 21, Part 177—Indirect Food Additives: Polymers, Electronic Code of Federal Regulations (eCFR), National Archives and Records Administration. Online [Accessed 22 June 2026]
https://www.ecfr.gov/current/title-21/chapter-I/subchapter-B/part-177
[34] L. M. Miller, J. P. Coates, Interpretation of infrared spectra: a practical and systematic approach, Encyclopedia of Analytical Chemistry (2025), pp. 1–24.
DOI: 10.1002/9780470027318.a5606.pub2
[35] R. Koningsveld, W. H. Stockmayer, E. Nies, Solid/liquid equilibrium, in: Polymer Phase Diagrams. Oxford University Press, Oxford, 2001, pp. 172–183.
DOI: 10.1093/oso/9780198556350.003.0012
[36] Y. Saruyama, Time dependence of the complex heat capacity at the melting temperature of polyethylene crystals, Thermochimica Acta 377 (2001), pp. 151–158.
DOI: 10.1016/S0040-6031(01)00550-0
[37] F. M. Mirabella, Crystallization and melting of a polyethylene copolymer: in situ observation by atomic force microscopy, Journal of Applied Polymer Science 108 (2008), pp. 987–994.
DOI: 10.1002/app.27739
[38] H. Widén, A. Leufvén, T. Nielsen, Migration of model contaminants from PET bottles: influence of temperature, food simulant and functional barrier, Food Additives and Contaminants Part A 21 (2004), pp. 993–1006.
DOI: 10.1080/02652030400009217
[39] M. R. Doran, P. Choi, Molecular dynamics studies of the effects of branching characteristics on the crystalline structure of polyethylene, J. Chem. Phys. 115, 2827–2830 (2001).
DOI: 10.1063/1.1386907
[40] D. Bamford, G. Dlubek, T. Lüpke, D. Kilburn, J. Stejny, T. J. Menke, M. A. Alam, Free volume, glass transition and degree of branching in ethylene/α-olefin copolymers: positron lifetime, differential scanning calorimetry, wide-angle X-ray scattering, and density studies, Macromolecular Chemistry and Physics 207 (2006), pp. 492–502.
DOI: 10.1002/macp.200500487
[41] R. A. Masumura, I. A. Ovid, Enhanced diffusion near amorphous grain boundaries in nanocrystalline and polycrystalline solids, Mater. Phys. Mech. 1 (2000), pp. 31–38. Online [Accessed 22 June 2026]
http://www.ipme.ru/e-journals/MPM/no_1100/paper6.pdf
[42] H. Kojima, K. Mukae, T. Yagasaki, N. Matubayasi, Dissolution and Diffusion of Small Molecules in the Amorphous and Crystalline States of Polymers Studied with All-Atom Molecular Dynamics, Macromulecules 58 (2025) 19.
DOI: 10.1021/acs.macromol.5c01679

SUPPLEMENTARY MATERIAL

Table S1: Combined DSC dataset of polyethylene packaging films

Sample ID	Onset (°C)	Peak Tm (°C)	End (°C)	ΔH_f (J/g)	%Xc (%)	Interpretation
PE-0001	110.92	121.29	128.67	74.41	25.4	PE (LDPE-like)
PE-0002	100.61	107.37	121.73	30.51	10.4	PE (LDPE-like)
PE-0003	114.4	121.9	129.78	44.96	15.3	PE (LDPE-like)
PE-0004	126.35	130.81	139.28	104.26	35.6	PE (HDPE-like)
PE-0005	95.26	120.66	129.1	92.79	31.7	PE (LDPE-like)
PE-0006	94.47	109.11	126.97	82.55	28.2	PE (LDPE-like)
PE-0007	122.82	129.24	139.31	136.69	46.6	PE (HDPE-like)
PE-0008	111.65	114.32 / 120.31	127.99	19.87	6.8	PE (LDPE-like)
PE-0009	122.24	129.26	139.89	142.13	48.5	PE (HDPE-like)
PE-0010	123.33	130.04	140.28	146.69	50.1	PE (HDPE-like)
PE-0011	123.28	129.77	139.97	145.49	49.6	PE (HDPE-like)
PE-0012	123	129.38	139.26	132.5	45.2	PE (HDPE-like)
PE-0013	123.51	130.01	138.77	136.62	46.6	PE (HDPE-like)
PE-0014	123.57	129.57	138.39	146.22	49.9	PE (HDPE-like)